American Journal of Biochemistry and Biotechnology

Research Article

Immunomodulatory and Antioxidant Activities of Selenium-Enriched Polysaccharides from Epimedium and Isatis Indigotica

Rui Zhang[1], Jin Li[2] and Jiajia Zhou[1]

[1]*School of Health, Jiangsu Vocational Institute of Commerce, Jiangsu 211168, China*
[2]*Department of Party Committee Organization, Jiangsu Vocational Institute of Commerce, Jiangsu, 211168, China*

Article history
Received: 17-01-2025
Revised: 31-05-2025
Accepted: 24-07-2025

Corresponding Author:
Rui Zhang
School of Health, Jiangsu Vocational Institute of Commerce, Jiangsu 211168, China
Email: ruizhang0103@163.com

Abstract: This study aims to investigate the effects of selenium modification on polysaccharides derived from two traditional Chinese medicinal herbs-Epimedium (Yinyanghuo) and Isatis root (Banlangen)-in enhancing immune function and antioxidant activity. The purpose is to explore the relationship between structure and function, providing a theoretical basis for the development of efficient plant-based functional antioxidants. Polysaccharides were extracted using an optimized enzymatic hydrolysis method and subsequently selenized using sodium hydrogen selenite, resulting in selenized Epimedium Polysaccharides (sEPS) and selenized Isatis Root Polysaccharides (sIRPS). Structural characterization was performed using infrared spectroscopy, UV spectroscopy, and thermogravimetric analysis. Antioxidant capacity was evaluated via ABTS radical scavenging assay, while immune-enhancing activity was assessed through Peripheral Blood Mononuclear Cell (PBMC) proliferation assays in vitro. The selenium modification retained the primary glycosidic backbone while enhancing both antioxidant and immunomodulatory activities. ABTS scavenging results showed that sIRPS samples achieved up to 35.26% clearance at 1 mg/mL concentration, with several samples maintaining high activity even at lower concentrations ($p<0.05$). PBMC proliferation experiments demonstrated that both sEPS and sIRPS significantly increased cell proliferation across multiple doses, with sIRPS7 showing the best performance in the medium-dose group ($p<0.05$). The selenium-modified polysaccharides from Epimedium and Isatis root exhibit significantly enhanced immune and antioxidant functions, with evident dose dependence. Unlike previous studies focusing on single-source selenium polysaccharides, this study establishes a comparative evaluation model under a unified experimental system, thereby expanding the application potential of organic selenium polysaccharides in functional foods and herbal therapeutics.

Keywords: Selenium, Polysaccharides, Immunogenicity, Antioxidant, Trace Element

Introduction

Selenium plays a vital physiological role in living organisms. It serves not only as an essential component of several key enzymes but also participates in numerous metabolic processes (Shi *et al.*, 2021). As a trace element necessary for human health, selenium is crucial for maintaining normal physiological functions, enhancing immune response, and ensuring overall well-being (Yang *et al.*, 2021). However, the bioavailability of selenium is relatively low, and its biological activity is significantly influenced by its chemical form, which poses a major challenge in current research (Abdel-Moneim *et al.*, 2022). In recent years, with the enhancement of people's health awareness and the improvement of living standards, functional foods, especially those rich in trace elements, have received widespread attention. Selenium-enriched foods, in particular, are being increasingly valued for their unique nutritional and health-promoting properties. Nevertheless, the limited absorption of

SCIENCE Publications

traditional selenium sources necessitates the development of new strategies to enhance selenium bioavailability and improve the quality of selenium-containing products (Wang *et al.*, 2021a). Polysaccharides are high-molecular-weight polymers composed of multiple monosaccharides or their derivatives linked by ether or glycosidic bonds (Ndwandwe *et al.*, 2021). They have attracted significant attention for their remarkable bioactivities, such as antioxidant, thermotolerant, and immunomodulatory effects (Ali *et al.*, 2021). Studies have shown that combining selenium with polysaccharides to form selenium-containing polysaccharides can significantly improve the stability and bioavailability of selenium (Zhao *et al.*, 2022). Polysaccharides have strong binding and encapsulation abilities, which enable them to form stable chemical bonds with selenium, thereby preventing its degradation and enhancing its biological functions (Zhang *et al.*, 2021). In addition, the encapsulation effect of polysaccharides can effectively prevent selenium from interacting with other substances, protect selenium, and improve its biological activity (Masood *et al.*, 2023). Therefore, this study starts from the perspective of selenium-containing polysaccharides.

This study selects Epimedium and Isatis root as sources of selenized polysaccharides based on their traditional medicinal value and existing research foundations. Epimedium has long been used for strengthening the body and nourishing essence, and its polysaccharides have been shown to possess strong immunomodulatory and antioxidant activities. Isatis root, commonly used for heat-clearing and detoxification, contains root-derived polysaccharides with notable free radical scavenging ability and immune cell activation effects. Compared with other medicinal plants, the research on polysaccharide structure and function of these two species is already very comprehensive. Therefore, Epimedium and Isatis root are suitable choices for exploring the enhancement of biological activity after selenium doping, and have the potential to develop functional foods or plant medicines.

The novelty of this study lies in the first systematic comparison of the immune enhancement and antioxidant activities of sEPS and sIRPS under the same experimental conditions. Combined with Fourier transform infrared spectroscopy, structural characterization is carried out, and a dual parameter activity evaluation strategy based on traditional Chinese medicine polysaccharides is established.

The contribution of this study is the establishment of a standardized extraction, purification, and selenization procedure for natural polysaccharides. Its significant effects on Peripheral Blood Mononuclear Cell (PBMC) proliferation and free radical scavenging are validated in vitro. This study provides experimental evidence and theoretical support for the development of these compounds as functional foods or botanical therapeutics.

In recent years, research on selenium-containing polysaccharides has gradually enriched. Yang *et al*. analyzed the improvement of biological activity of selenium polysaccharides. However, due to their low selenium content, the geographical scope of their acquisition was limited. Therefore, the development of organic selenium polysaccharides with high selenium content has become a research hotspot to enhance the biological activity of selenium polysaccharides. These research results had significant implications for the future development and utilization of selenium polysaccharides in health or medical care. Overall, there has been some research progress in the sources, preparation methods, and biological activities of selenium polysaccharides (Yang *et al.*, 2021). Zhang *et al.* (2022) used GC-MS and 2D NMR techniques to conduct a detailed study on the chain structure of the natural selenium polysaccharide Selenium-enriched Polygonatum odoratum polysaccharide fraction 3 (Se-POP-3), while also exploring its anti-gastric and colon cancer effects. The research results showed that Se-POP-3 could reduce the survival rate of human gastric carcinoma cell line MGC-803 and human colorectal carcinoma cell line HCT-116 cells, induce cell apoptosis, inhibit cell migration and invasion, destroy Ratio of Bcl-2-associated X protein to B-cell lymphoma 2 protein (Bax/Bcl-2 ratio), and inhibit epithelial mesenchymal transition. In addition, the study also found that within the set concentration range, Se-POP-3 had no significant effect on the growth of Normal Colon Mucosal epithelial cell line 460 (NCM460) cells. This study provided a theoretical basis for the potential application of Se-POP-3 as an anti-gastric and colon cancer drug or functional food. Tang *et al.* (2021) successfully prepared uniformly dispersed and stable selenium nanoparticles (SeNPs) using a simple redox process of selenate and ascorbic acid using ganoderma lucidum polysaccharides (GLPs) as stabilizers and dispersants. They used various detection techniques such as dynamic light scattering, electron microscopy, and X-ray analysis to comprehensively analyze the size, stability, morphology, and physicochemical properties of GLPs SeNPs. Research has found that GLPs SeNPs exhibited an orange-red color, amorphous, zero-valent, and spherical shape, with an average diameter of approximately 92.5 nm, and exhibited good stability at 4°C, different ion strengths, and pH environments. In addition, the study also found that GLPs SeNPs had excellent antioxidant capacity, which could effectively inhibit the activities of α-amylase and α-glucosidase compared to bare tellurium nanoparticles, GLPs, and sodium tellurate. The in vitro toxicity test and hemolytic activity test results indicated that GLPs SeNPs had good biocompatibility. Therefore, GLPs SeNPs had the potential to be used as antioxidants and anti-diabetes agents in food and medicine. Gharibzahedi *et al.* (2022) used a new solvent extraction method that combines ultrasound and microwave-assisted

extraction of polysaccharides and studied their resistance to tumors. Through purification, classification, and biological analysis, research has identified some polysaccharide fragments with strong anti-proliferative, anti-tumor, and anticancer effects. It also found that these polysaccharides caused morphological changes related to cell death, thereby inhibiting the growth of human cancer cells. In addition, substances such as polysaccharides, galactose, and pectin had no toxicity to normal cells. Instead, they exhibited anti-tumor potential by inducing cell apoptosis and inhibiting tumor occurrence, metastasis, and deformation. There was a high correlation between anti-proliferative activity and the structural characteristics of extracted polysaccharides (such as molecular weight, monosaccharide composition, sulfate, selenium, uric acid content, etc.) and other biological functions (such as anti-free radicals and antioxidant). Studying the structure-activity relationship of anti-tumor polysaccharides was of great significance for the development of efficient anti-cancer drugs and foods, without producing any side effects.

In addition, research on immune enhancement and antioxidant activity has also made progress. Chen *et al.* (2023) developed a novel curcumin-related polyester to increase the stability and solubility of curcumin in physiological environments. This polyester is formed by combining curcumin with the polymer main chain under the action of polyethylene glycol and decanoyl chloride. Its properties, including thermal and mechanical properties, surface wettability, self-assembly behavior, and drug release kinetics, are closely related to the curcumin content in the polymer. In addition, the release rate of curcumin can be controlled through the hydrolysis reaction of phenolic esters on the main chain of the polymer, which is related to the hydrophilicity of the polymer. Researchers have found that these materials have efficient antioxidant and neuroprotective properties, and can be made into various forms such as thin films and self-assembled particles. Therefore, there is reason to believe that these materials have broad application prospects in fields such as neural tissue engineering. Angelo *et al.* (2022) conducted in-depth research on the bioactive substances in plants, i.e., phenolic compounds. They paid special attention to the content of phenolic compounds in Coffea canephora's roasted beans, including caffeic acid, chlorogenic acid, and phenolic acid. By using high-performance liquid chromatography, it was found that in 100 grams of dry matter, the content of caffeic acid was 3.7%, chlorogenic acid was 5.4%, and phenolic acid was 2.8%. In addition, they also measured the antioxidant activity, as well as the content of total phenols and flavonoids in the plant seeds. The results showed that the concentration of 50% inhibition of 2, 2-Diphenyl-1-Picrylhydrazyl (DPPH) free radicals was 75.54±2.08 μg/mL, and the contents of total phenols and flavonoids were 81.67 mg EAG/g and 293.33 mg EQ/g, respectively. Researchers believe that this antioxidant activity may be related to the abundance of phenolic compounds in this plant seed. These results provide useful insights into the possibility of using natural compounds as antioxidants, which may have no side effects and can replace chemically synthesized antioxidant molecules. Shabana and Abd El-Sadek (2021) aimed to use carbomer as an adjuvant to enhance the immunogenicity of the trivalent foot-and-mouth disease vaccine, thereby providing high protection and long-term immunity against foot-and-mouth disease. They chose guinea pigs as experimental models because they are not only the most cost-effective animal models but also have clinical symptoms similar to those of pigs and cows, making them an ideal model for developing and testing the foot-and-mouth disease vaccine PD50. They prepared three different formulations of inactivated trivalent foot-and-mouth disease vaccines, including O Pan Asia2, A Iran O5, and SAT2/EGY/2012 serotypes. All of these formulas have not detected any foreign pollutants, are safe and effective, and can produce high levels of foot-and-mouth disease specific antibodies in guinea pigs. The immunogenicity of various vaccine formulations was determined by evaluating the protective dose of 50% (GPPD50) in guinea pigs and monitoring the humoral antibody response of vaccinated guinea pig populations. Research has shown that vaccine formulations using Montanide 206 oil and carbopol as adjuvants had the best efficacy, followed by Montanide 206 oil and carbopol, which can provide early short-term immunity.

In summary, current research has demonstrated the potential of selenized polysaccharides in enhancing immune function, antioxidant activity, and tumor inhibition, with such effects closely linked to their structural characteristics. However, most existing studies focus on single sources or specific types of selenized polysaccharides, lacking systematic comparisons across different herbal sources under unified experimental conditions. Moreover, the mechanisms underlying the enhancement of biological functions through selenization remain inadequately explored. This study prepared selenized polysaccharides by selecting Epimedia and Isatis root, two widely used medicinal and edible herbaceous plants. Its immune regulation and antioxidant properties have been compared and evaluated, aiming to deepen the understanding of its structure-function relationship and provide support for its application in functional foods or plant medicine.

Unlike previous studies that mainly focused on inorganic selenium or nano-selenium, this study utilizes organic selenium to modify natural medicinal polysaccharides. This approach balances biocompatibility and functional controllability while avoiding potential toxicity or stability issues of traditional selenium materials. Establishing a unified multi-source comparative analysis experimental platform can help to

more comprehensively elucidate the relationship between the structure and biological effects of selenium polysaccharides. This study can provide new insights into the safe and sustainable application of such compounds.

Methods

This study first prepared Epimedium polysaccharides (EPS) and Isatis Root Polysaccharides (IRPS) through the herbal extraction process, and purified and selenified them. Subsequently, the content of polysaccharides and selenium was determined using the sulfuric acid phenol method and the vaporization generation atomic fluorescence spectrometry, respectively. Finally, the polysaccharides were identified using infrared spectroscopy. In the immune enhancement test, the study compared the effects of selenized Epimedium polysaccharides (sEPS) and selenized Isatis root polysaccharides (sIRPS) on PBMC, and determined their maximum safe concentration and concentration range for enhancing immune activity. In the antioxidant activity test, methods such as DPPH free radical scavenging test, hydroxyl free radical capacity measurement, and ABTS free radical scavenging test were used to compare the antioxidant capacity of two polysaccharides.

Chemicals and Instruments

All reagents used in this study were of analytical grade unless otherwise specified. Phenol and concentrated sulfuric acid were purchased from Sinopharm Chemical Reagent Co., Ltd. (China). Sodium selenite (Na_2SeO_3) was obtained from Macklin Biochemical Co., Ltd. (China) and absolute ethanol was purchased from Tianjin Kermel Chemical Reagent Co., Ltd. (China). RPMI-1640 medium was supplied by Gibco, Thermo Fisher Scientific (USA), while phytohemagglutinin (PHA) and ABTS were obtained from Sigma-Aldrich (USA). Heparin sodium was sourced from Solarbio Life Sciences (China), 3-(4,5-Dimethylthiazol-2-yl)-2,5-Diphenyltetrazolium Bromide (MTT) reagent was obtained from from Beyotime Biotechnology (China), and hydrogen peroxide and ferrous sulfate was obtained from Aladdin Reagent Co., Ltd. (China).

The main instruments used in the experimental procedures included: A UV-visible spectrophotometer (UV-2600, Shimadzu, Japan) for absorbance measurements; a hydride generation atomic fluorescence spectrometer (AFS-2202E, Haiguang Instrument Co., Ltd., China) for selenium content analysis; a Fourier transform infrared spectrometer (Tensor II, Bruker, Germany) for structural characterization. A freeze dryer (LGJ-10, Boyikang, China) was used to obtain dried polysaccharide samples. Cell viability and proliferation were measured using a microplate reader (Infinite M200 PRO, Tecan, Switzerland), and morphological observations were performed with an inverted microscope (CKX53, Olympus, Japan). Additionally, a constant temperature incubator (MJX-160B, Boxun, China), a mini orbital shaker (THZ-100, Taicang Experimental Instrument Factory, China), and an analytical balance (AL204, Mettler Toledo, Switzerland) were utilized throughout the study.

Plant Materials

The Epimedium and Isatis root decoction pieces used in this study were purchased from Nanjing Jinling Pharmacy (Jiangsu Province, China). The Epimedium samples were produced by Anhui Jiren Co., Ltd. (Batch No. 12067), and the Isatis root samples were provided by Xuzhou Pengzu Traditional Chinese Medicine Co., Ltd. (Batch No. 12067). Both herbal materials were stored in a dry and ventilated environment prior to use. The authenticity of the materials was verified according to the standards of the Chinese Pharmacopoeia (2020 Edition).

Preparation of Selenium-Containing Polysaccharides

Polysaccharides from Epimedium and Isatis root were prepared through a standardized herbal extraction process. 2 kg of the dried aerial parts of Epimedium and 2 kg of the dried roots of Isatis root were pulverized and passed through a fine-mesh sieve. The powdered materials were extracted with 10 times their volume of distilled water by refluxing in a water bath at 85℃ for 2 h/cycle, repeated 3 times. The combined filtrates were obtained by gauze filtration and concentrated to 1/5 of the original volume using a rotary evaporator under reduced pressure at 50℃ (Sun *et al.*, 2024). The concentrated extract was mixed thoroughly with 95% ethanol at a volume ratio of one to three and left to stand at 4℃ for 24 hours to precipitate polysaccharides (Fan *et al.*, 2022). The resulting precipitate was collected by centrifugation at 8,000 revolutions per minute for 10 minutes, washed 3 times with absolute ethanol, and freeze-dried to obtain the crude polysaccharide samples.

Protein impurities were removed using the Sevag method. Specifically, the crude polysaccharide solution was mixed with chloroform and n-butanol at a volume ratio of four to one, vigorously shaken for 10 minutes, and allowed to stand until phase separation occurred. The upper aqueous layer was retained, and the process was repeated 4 times to ensure complete deproteinization (Zhang and Huang, 2022). The deproteinized polysaccharide solution was then purified by ion exchange chromatography using a Diethylaminoethyl cellulose 52 (DEAE-52) cellulose column. Gradient elution was performed with Tris-HCl buffer solutions containing 0.1 molar and 0.3 molar sodium chloride at a pH of 7.2 (Wang *et al.*, 2021b). The elution rate is controlled at 1 mL/min. The eluted fractions containing polysaccharides were collected, concentrated, precipitated with ethanol, and freeze-dried to obtain the

purified Epimedium polysaccharide and Isatis root polysaccharide.

Based on this, selenization of the purified polysaccharides was carried out. 100 mg of purified polysaccharide were dissolved in 50 ml of distilled water, and 10 ml of sodium selenite solution at a concentration of 0.5 mg/ml were added (Ma *et al.*, 2022). The mixture was stirred in a three-necked flask and maintained at 50°C for 6 hours. During the reaction, 0.5 molar sodium carbonate solution was slowly added to adjust the pH to 8.0 to stabilize the reaction system. After completion, the solution was naturally cooled and transferred to a dialysis bag with a molecular weight cut-off of 3500 Daltons, and dialyzed in distilled water for 48 hours to remove small-molecule impurities. The dialyzed solution was then freeze-dried to obtain sEPS and sIRPS, which were used in subsequent bioactivity evaluations.

The polysaccharide content was determined using the phenol-sulfuric acid method (Plermjai *et al.*, 2023). D-(+)-glucose was used as the standard to prepare standard solutions with concentrations of 0, 20, 40, 60, 80, and 100 mcg/ml for the construction of the calibration curve. Specifically, 0.5 ml of the sample solution was added to a colorimetric tube, followed by 0.5 ml of 5% phenol solution. Then, 2.5 ml of concentrated sulfuric acid was added rapidly, and the mixture was thoroughly shaken. After the reaction mixture was left to stand at room temperature for 30 minutes to develop color, the absorbance was measured at 490 nm using a UV-visible spectrophotometer. The glucose concentration was plotted on the x-axis and the absorbance on the y-axis to generate a standard curve, and the polysaccharide content in the samples was calculated accordingly. Figure 1 shows the preparation process.

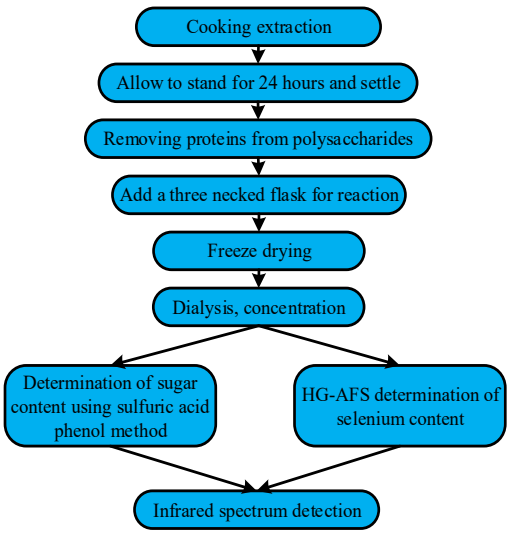

Fig. 1: Preparation process
Note: This figure illustrates the overall preparation process of sEPS, including cooking extraction, protein removal, freeze-drying, dialysis, and subsequent detection methods such as sulfuric acid phenol assay, HG-AFS for selenium determination, and infrared spectroscopy.

The determination of selenium content is carried out using hydride generation-atomic fluorescence spectrometry (HG-AFS). The sEPS and sIRPS are first dissolved in distilled water, and then concentrated in a triangular flask. Afterwards, acidic media was added to remove impurities, interference such as bubbles was reduced through centrifugation, and further concentration and drying were carried out. Finally, the selenium content in the sample was determined by detecting fluorescence intensity. Finally, infrared spectroscopy was used to detect the purified polysaccharides within the range of 4000-400 cm^{-1} to confirm the degree of purification of sEPS and sIRPS. In spectral analysis, a mixture of sealing mud and polysaccharides was made into transparent and uniform compression plates, which were then measured in a Fourier transform infrared spectrometer. By analyzing the infrared spectrum, the composition and structure of polysaccharides can be identified. Throughout the entire process, attention should be paid to many factors and details, such as strict control of time and temperature when cooking and extracting polysaccharides from Epimedium and Isatis root. When modifying with selenium, it was necessary to choose an appropriate amount of sodium selenite to effectively increase the content of polysaccharides. When using infrared spectroscopy for detection, attention should be paid to the selection of window materials to achieve good transmittance and resolution. The extraction rate of polysaccharides Q is show in formula (1):

$$Q = DG / BG \times 100\% \tag{1}$$

In formula (1), DG represents the mass of polysaccharides. BG represents the quality of Isatis root. When conducting polysaccharide identification, the concentration of the reference substance is taken as the horizontal axis X, and the absorbance is taken as the vertical axis Y. The response equation is formed according to formula (2):

$$\begin{cases} Y = Ax + b \\ Z = R^2 \end{cases} \tag{2}$$

Immunoenhancement Test

The experiment aimed to compare the in vitro immunoenhancing effects of sEPS and sIRPS on PBMCs, thereby identifying natural polysaccharide compounds with stronger immune-enhancing potential. PBMCs were isolated from fresh anti-coagulated blood obtained from

healthy adult volunteers in the laboratory. The separation was performed using Ficoll density gradient centrifugation. All procedures complied with ethical requirements and were conducted with informed consent from the participants. The isolated PBMCs were re-suspended in complete Roswell Park Memorial Institute-1640 Medium (RPMI-1640) medium and adjusted to a concentration of 1×10^6 cells/ml. A total of 100 microliters of cell suspension was seeded into each well of a 96-well plate. Experimental and control groups were established. The experimental groups were treated with sEPS or sIRPS at concentrations of 25, 50, 100, and 200 mcg/ml. The control groups included a blank cell control and a positive control treated with phytohemagglutinin. Each group was set up in triplicate and incubated for 48 hours in a humidified incubator at 37°C with 5% carbon dioxide.

Cell proliferation was assessed using the MTT assay. Ten microliters of MTT solution at a concentration of 5 mg/ml was added to each well and incubated for an additional 4 hours. After discarding the supernatant, 150 microliters of dimethyl sulfoxide was added to dissolve the formazan crystals. The solution was shaken thoroughly, and the absorbance was measured at 570 nn using a microplate reader. The proliferation rate was calculated based on the absorbance values relative to the blank control group. The experimental results were used to evaluate the proliferative effects of different concentrations of polysaccharides on PBMC and to determine their maximum safe concentration, which was defined as maintaining a cell viability above 90%. Instruments used in this experiment included a microplate reader, inverted microscope, constant-temperature incubator, and microplate shaker. Major reagents used included complete RPMI-1640 medium, phytohemagglutinin, heparin sodium anticoagulant, and MTT dye, all of which were high-quality analytical-grade products. Figure 2 shows the specific process.

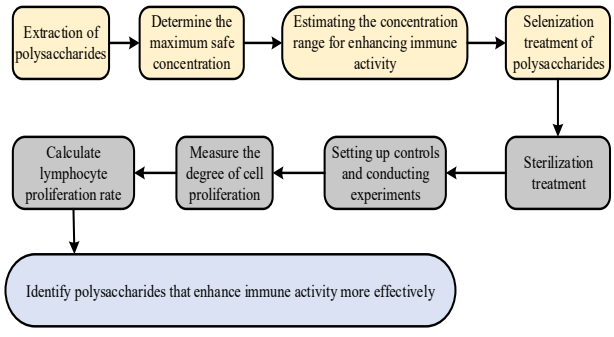

Fig. 2: Immunoenhancement Test

Note: This figure illustrates the immunological experimental procedure used to evaluate the immune-enhancing effects of selenized polysaccharides, including maximum safe concentration determination, immune activity range estimation, lymphocyte proliferation testing, and identification of polysaccharides with optimal immune stimulation capacity.

Antioxidant Activity Test

To evaluate the antioxidant activity of sEPS and sIRPS, three free radical scavenging assays were employed, including the DPPH (2, 2-diphenyl-1-picrylhydrazyl) radical scavenging assay, the hydroxyl radical scavenging assay, and the ABTS (2, 2′-azino-bis (3-ethylbenzothiazoline-6-sulfonic acid) radical scavenging assay. The experimental procedure is shown in Figure 3.

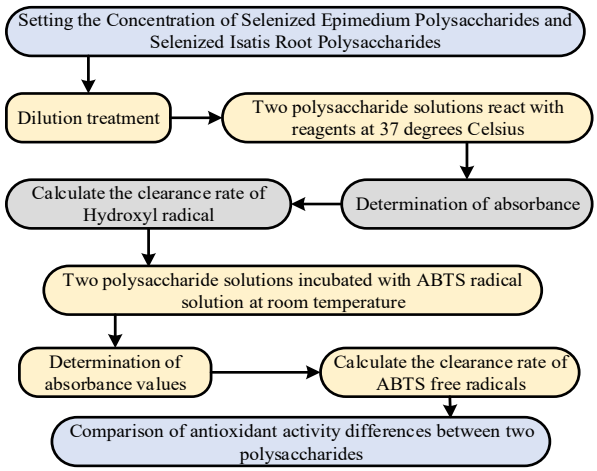

Fig. 3: Antioxidant activity test

Note: This figure presents the experimental procedure used to evaluate the antioxidant capacity of sEPS and sIRPS, including dilution, radical scavenging tests with hydroxyl and ABTS radicals, absorbance measurements, and comparative analysis of antioxidant activity.

First, according to the experimental design, the two selenium-enriched polysaccharide samples were diluted to the designated concentrations of 25, 50, 100, and 200 mcg/ml. The DPPH radical scavenging assay was performed according to the method of Brand-Williams. A 0.1 millimolar DPPH ethanol solution was mixed with an equal volume of polysaccharide solution, and the mixture was incubated in the dark at room temperature for 30 minutes. The absorbance was then measured at 517 nm to calculate the DPPH scavenging rate (Desale *et al.*, 2021). In the hydroxyl radical scavenging assay, the polysaccharide solution was mixed with $FeSO_4$, H_2O_2, and salicylic acid and incubated at 37°C for 30 minutes. The absorbance was then measured at 510 nm, and the hydroxyl radical scavenging rate was calculated. The vitamin C (Vc) group served as the positive control (Ge *et al.*, 2023). The calculation of hydroxyl radical scavenging rate K_1 follows formula (3):

$$K_1 = [1 - A_x / A_0] \times 100\% \quad (3)$$

In formula (3), A_x represents the absorbance of polysaccharides and *Vc* groups, and A_0 represents the absorbance of the control group. In the ABTS radical scavenging assay, the ABTS working solution was first prepared by reacting ABTS with potassium persulfate for 12-16 hours. The resulting solution was diluted until the initial absorbance at 734 nm reached 0.70±0.02. Then, 1 ml of the diluted ABTS solution was mixed with 1 ml of polysaccharide solution at various concentrations, incubated at room temperature for 6 minutes, and the absorbance was measured at 734 nm (Kulkarni and Govindaiah, 2022). The ABTS radical scavenging rate K_2 is then calculated using formula (4):

$$K_2 = [1 - A'_x / A'_0] \times 100\% \quad (4)$$

In formula (4), A'_0 represents the absorbance of the polysaccharide and *Vc* groups, while A'_0 represents the absorbance of the control group.

Results

The study first conducted experimental studies on Epimedium and Isatis root, extracting and purifying their selenium containing polysaccharides. The polysaccharides in Epimedium and Isatis root were extracted by water decoction and alcohol precipitation methods. For the immuneenhancement effect of selenium-containing polysaccharides, this study set up two different experimental environments: One type is to stimulate lymphocytes separately with sEPS and sIRPS; Another type is to utilize the synergistic effect of sEPS and sIRPS on PHA to stimulate lymphocyte proliferation. The proliferative effects of sEPS and sIRPS on lymphocytes were evaluated by recording and analyzing the A570 and MTT values of lymphocytes. Among them, A570 represents the absorbance value measured at a wavelength of 570 nm. For the experimental analysis of antioxidant activity, this study evaluated their antioxidant activity by measuring the scavenging ability of sEPS and sIRPS on hydroxyl and ABTS radicals. The hydroxyl radical and ABTS radical scavenging rates of various polysaccharide samples at different concentrations were recorded and compared in detail, thereby identifying the differences and patterns in their antioxidant activity.

Preparation Experiment of Selenium-Containing Polysaccharides

This study processed Epimedium and Isatis root with water decoction and alcohol precipitation, extracted polysaccharides, and analyzed the structure and properties of selenide polysaccharides using infrared spectroscopy. As shown in Table 1, this study observed the characteristic vibrational peaks to gain a deeper understanding of the structure and properties of selenide polysaccharides.

In Table 1, sEPS type 1 has a higher yield and moderate sugar and protein content, indicating a relatively good extraction and purification process. The yield of sEPS type 2 is lower than that of sIRPS type 2, but it has high sugar content and low protein content, indicating a higher extraction purity. The output rate of sIRPS Type 3 is moderate. The elution curve is shown in Figure 4.

In Figure 4, two extraction and purification methods for polysaccharides were obtained through experimental research on Epimedium and Isatis root. Firstly, 2 kg of Epimedium were processed by decoction and alcohol precipitation, resulting in a total EPS mass of 84.69 g, with an incidence rate of 4.24%. In addition, the sugar content of Epimedium was 21.35%. Then, two peaks were separated using DEAE-52 cellulose chromatography washing method, and these two peaks were collected separately to obtain two purified EPS 1 and EPS 2. After measurement, the polysaccharide content of EPS 1 and EPS 2 was 53.1% and 37.34%, respectively. The same steps were also applicable to the decoction pieces of Isatis root. After being treated with water decoction and alcohol precipitation, the total IRPS t of Isatis root obtained was 104.76 g, with a yield of 5.24%. Isatis root had a higher sugar content, reaching 34.76%. Next, further purification needed to be carried out using DEAE-52 cellulose column chromatography elution method. After obtaining two peaks, the study obtained two purified polysaccharides IRPS1 and IRPS2 from Isatis root. The content of these two polysaccharides was determined and it was found that the polysaccharide contents of IRPS1 and IRPS2 were 97.92% and 30.85%, respectively. The infrared spectrum is shown in Figure 5.

Table 1: Structure and properties of selenide polysaccharides

Polysaccharide type	Yield (%)	Sugar content (%)	Protein (%)
sEPS Type 1	4.38	21.58	1.45
sEPS Type 2	1.56	52.67	0.57
sEPS Type 3	1.72	37.11	0.66
sIRPS Type 1	5.38	34.8	2.85
sIRPS Type 2	2.05	97.45	0.37
sIRPS Type 3	4.75	30.95	0.8

Note: Table 1 shows the extraction yield, sugar content, and protein content of different types of selenized polysaccharides derived from sEPS and sIRPS. These data reflect the efficiency and purity of the extraction and purification processes for each polysaccharide type

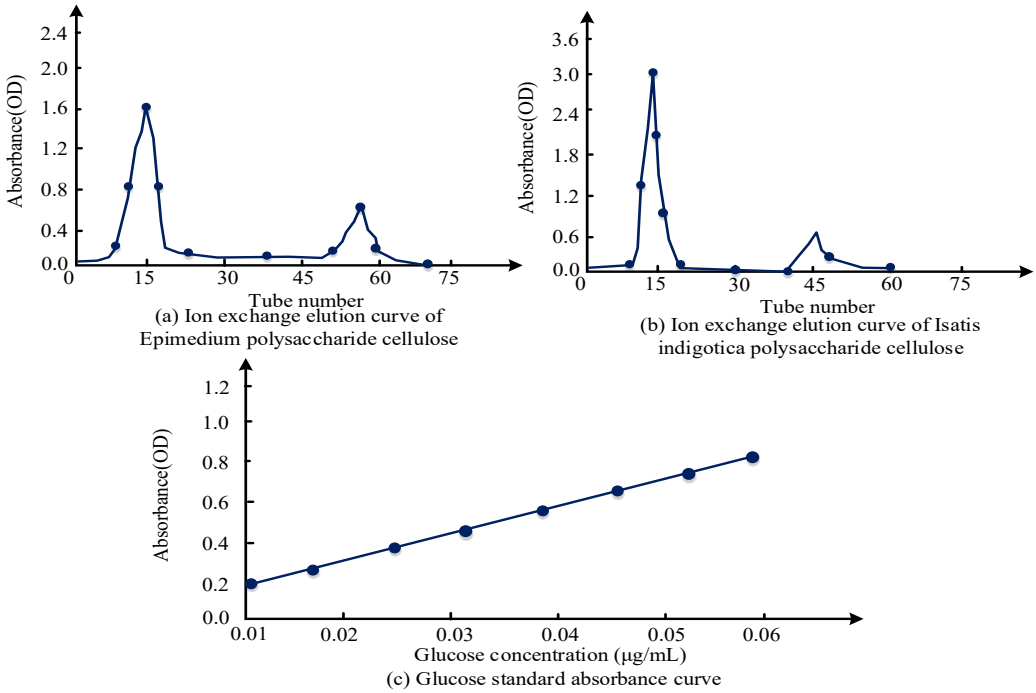

Fig. 4: Elution curve and absorbance curve

Note: This figure includes three parts: (a) the elution curve of sEPS obtained from DEAE-52 ion exchange chromatography, (b) the elution curve of sIRPS under the same chromatographic conditions, and (c) the standard curve of D-(+)-glucose concentration versus absorbance at 490 nm, used to quantify polysaccharide content by the sulfuric acid-phenol method

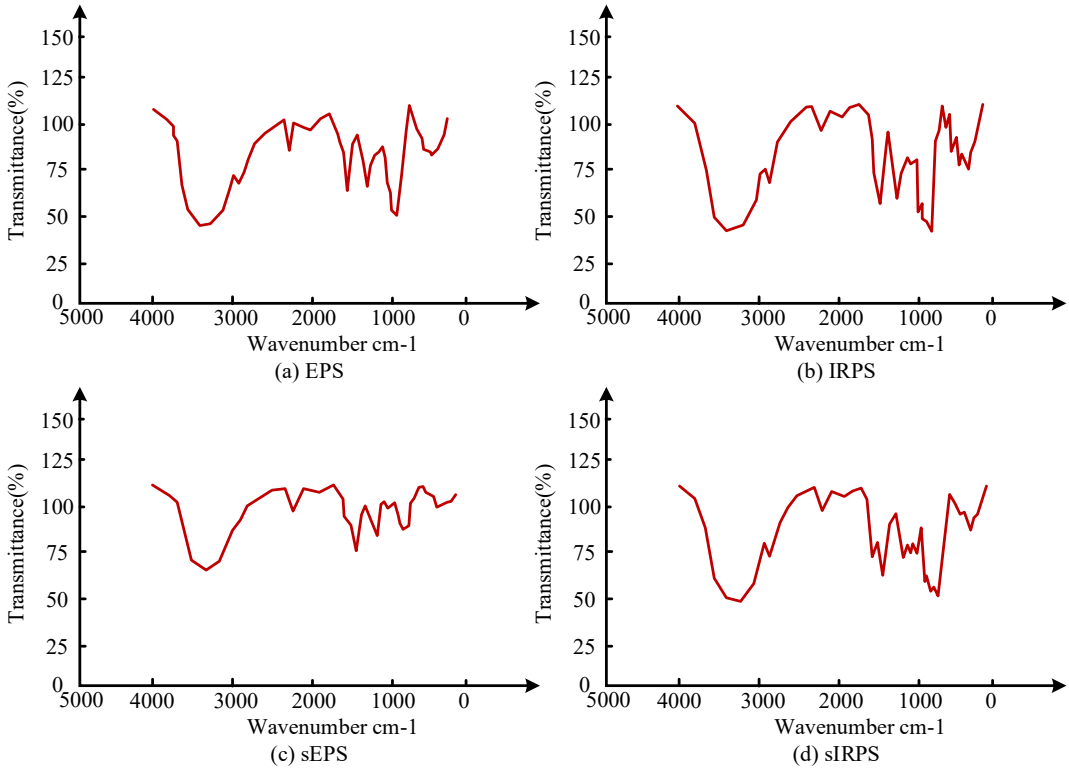

Fig. 5: Infrared spectrum

Legend: This figure presents the FTIR spectra of four polysaccharide samples: (a) EPS, (b) IRPS, (c) sEPS, and (d) sIRPS. Characteristic absorption peaks corresponding to functional groups such as hydroxyl, carboxyl, and glycosidic bonds are observed, supporting structural identification and comparison before and after selenization.

In Figure 5, the infrared spectrum of selenide polysaccharides played an important role in the analysis. In the infrared spectra of EPS and IRPS, some characteristic vibrational peaks of sugars could be observed. Specifically, EPS had a strong and broad absorption peak at the position of 3363.16 cm^{-1} and IRPS at the position of 3387.74 cm^{-1}, which was considered a manifestation of the stretching vibration of the hydroxyl (O–H) bond. In addition, EPS had an absorption peak at the position of 1637.89 cm^{-1} and IRPS at the position of 1642.52 cm^{-1}, which was considered a manifestation of tensile vibration with carbonyl (C = O). At positions 1,400-1,000 cm^{-1}, absorption peaks of C-H, C-O, and C-C vibrations could be observed. The infrared spectra of sEPS and sIRPS also exhibited similar characteristics. The characteristic vibrational peaks of these infrared spectra provided key information on selenide polysaccharides. These characteristic absorption peaks indicated that the selenized polysaccharides retained the fundamental backbone structure of the original polysaccharides, while undergoing localized molecular adjustments during the selenization process. For example, the slight shifts and changes in intensity of the O–H peak suggested its potential involvement in bonding with selenium. The enhancement in the C=O vibration region might be associated with the introduction of selenium groups, leading to a new polar environment. Moreover, the unchanged C–O and C–C vibration signals indicated that the glycosidic backbone remained structurally intact. Collectively, these results demonstrated that selenium has been successfully incorporated into the polysaccharide molecules without disrupting the main chain structure, thereby endowing the compounds with new physicochemical properties.

Analysis of Immune Enhancement Test

As shown in Table 2, in the immune enhancement test, the study first measured the A570 values of lymphocytes in each group when stimulated by sEPS alone.

Table 2: The absorbance values at 570 nm (A570) of lymphocytes in each group when individually stimulated with sEPS

Concentration (μg/mL)	1.563	0.782	0.391	0.196	0.098	Cell control
sEPS1	0.162±0.007	0.169±0.008	0.177±0.009	0.187±0.008	0.189±0.007	0.156±0.007
sEPS2	0.176±0.007	0.189±0.007	0.208±0.006	0.190±0.007	0.191±0.008	0.159±0.006
sEPS3	0.159±0.009	0.179±0.006	0.174±0.007	0.185±0.006	0.185±0.007	0.158±0.007
sEPS4	0.166±0.007	0.185±0.005	0.182±0.006	0.191±0.006	0.203±0.006	0.154±0.006
sEPS5	0.176±0.004	0.191±0.007	0.186±0.007	0.200±0.005	0.195±0.007	0.151±0.006
sEPS6	0.191±0.008	0.198±0.009	0.214±0.008	0.223±0.007	0.227±0.008	0.185±0.008
sEPS7	0.219±0.007	0.240±0.008	0.242±0.007	0.246±0.006	0.258±0.007	0.215±0.007
sEPS8	0.155±0.006	0.158±0.007	0.168±0.006	0.183±0.007	0.198±0.006	0.143±0.006
sEPS9	0.162±0.007	0.169±0.008	0.171±0.007	0.174±0.006	0.188±0.007	0.157±0.007
EPS(pg.mL)	0.176±0.006	0.181±0.007	0.182±0.008	0.184±0.007	0.170±0.006	0.167±0.006

Note: Table 2 presents the absorbance values at 570 nm (A570) of lymphocytes in each group when individually stimulated with different types and concentrations of sEPS. The results reflect the proliferation response of lymphocytes under various dosages, with the cell control group serving as a negative control

As shown in Table 2, the study showed the effect of different concentrations of sEPS (sEPS1-sEPS9) on lymphocyte proliferation. Firstly, the lymphocyte proliferation in the control group was 0.156~0.167±0.006. At different concentrations, the value-added effect of sEPS on lymphocytes varied. For sEPS1, when the concentration increased from 1.563 μg/mL to 0.098 μg/mL, lymphocyte proliferation increased from 0.162±0.007 to 0.189±0.007, reflecting a gradual increase in lymphocyte proliferation under the stimulation of higher concentrations of sEPS. However, the promotion effect of the highest concentration on lymphocyte proliferation might not be the most significant. For sEPS2, it achieved a maximum increase of 0.208±0.006 at a concentration of 0.391 μg/mL. For sEPS6 and sEPS7, as the concentration increased, lymphocyte proliferation increased significantly. At the concentration of 0.098 μg/mL, the increment of sEPS6 and sEPS7 reached 0.227±0.008 and 0.258±0.007, respectively, which were higher than the control group level (p<0.05 indicates that the result is significant). From sEPS1 to sEPS9, the proliferation of lymphocytes showed a certain trend of change. At a concentration of 1.563 μg/mL, the lymphocyte proliferation of sEPS7 was the highest at 0.219±0.007, while sEPS8 was the lowest at 0.155±0.006. At other concentrations, sEPS7 also had the highest lymphocyte proliferation. This indicated that sEPS7 had a better effect on lymphocyte proliferation than other polysaccharides. Through comparison, it was evident that there were differences in the effects of different sEPS on lymphocyte proliferation. Their respective optimal stimulation concentrations also varied. On this basis, a more in-depth study of the biological activity and application value of different sEPS was of great significance

for understanding how they regulate immune function. Table 3 shows the changes in lymphocyte proliferation during the synergistic effect of sEPS on PHA stimulation.

In Table 3, the study conducted in-depth research and exploration on the changes in lymphocyte proliferation under the synergistic effect of sEPS on PHA stimulation, and obtained some meaningful data and results. Firstly, based on the experimental data of the study, for lymphocytes with a concentration of 1.580, the MTT value range of sEPS (sEPS1-sEPS5) was between 0.315±0.007 and 0.335±0.004. Among them, sEPS2 performed best with a value of 0.342±0.009. However, compared with the control group (PHA, cell control), their values were significantly higher, indicating that sEPS successfully stimulated lymphocyte proliferation (p<0.05 indicates that the result is significant). Secondly, when the concentration dropped to 0.789, the MTT value of lymphocytes under the action of sEPS (sEPS1-sEPS5) decreased, but it remained stable and has a high value. Especially for sEPS2 and sEPS5, the values were still as high as 0.344±0.003 and 0.345±0.006. This once again reflected the strong effect of sEPS on stimulating lymphocyte proliferation. At the same time, when the concentration decreased to 0.397, 0.200, and 0.100, sEPS (sEPS1-sEPS5) further stimulated lymphocyte proliferation, leading to a significant increase in MTT values. For example, at a concentration of 0.100, the MTT values of sEPS2 and sEPS5 increased to 0.376±0.003 and 0.394±0.004, respectively. Surprisingly, these values have far exceeded those of the control group, and their increase is increasing, indicating that the effect of sEPS on stimulating lymphocyte proliferation increases with the decrease of concentration. Table 4 shows the changes in lymphocyte proliferation induced by sIRPS alone.

Table 3: Changes in lymphocyte proliferation during synergistic PHA stimulation with sEPS

Concentration(μg/mL)	1.563	0.782	0.391	0.196	0.098	PHA	Cell control
sEPS1	0.315±0.007	0.310±0.006	0.320±0.005	0.328±0.005	0.339±0.007	0.300±0.007	0.235±0.006
sEPS2	0.342±0.009	0.344±0.003	0.352±0.002	0.358±0.003	0.376±0.003	0.310±0.009	0.229±0.006
sEPS3	0.314±0.008	0.310±0.005	0.307±0.006	0.319±0.004	0.328±0.002	0.294±0.006	0.228±0.006
sEPS4	0.337±0.007	0.335±0.006	0.335±0.007	0.346±0.004	0.357±0.001	0.326±0.007	0.220±0.004
sEPS5	0.335±0.004	0.345±0.006	0.368±0.003	0.378±0.004	0.394±0.004	0.310±0.004	0.222±0.007
sEPS6	0.336±0.005	0.342±0.005	0.351±0.003	0.350±0.004	0.359±0.006	0.323±0.006	0.226±0.005
sEPS7	0.310±0.007	0.318±0.007	0.320±0.005	0.323±0.005	0.334±0.005	0.291±0.007	0.234±0.006
sEPS8	0.328±0.006	0.336±0.006	0.338±0.006	0.352±0.006	0.370±0.006	0.298±0.008	0.229±0.003
sEPS9	0.303±0.009	0.312±0.008	0.323±0.008	0.330±0.010	0.337±0.006	0.292±0.006	0.228±0.009
EPS	0.318±0.006	0.324±0.005	0.325±0.004	0.342±0.007	0.349±0.006	0.303±0.007	0.237±0.005

Note: Table 3 shows the absorbance values at 570 nm (A570) of lymphocytes when co-stimulated with PHA and different concentrations of sEPS. The data reflect enhanced lymphocyte proliferation under synergistic immune stimulation. PHA-stimulated cells served as a positive control, and unstimulated cells served as a negative (cell) control

Table 4: Changes in lymphocyte proliferation induced by sIRPS alone

Concentration(μg/mL)	1.563	0.782	0.391	0.196	0.098	Cell control
sIRPS1	0.200±0.004	0.212±0.008	0.224±0.005	0.212±0.006	0.220±0.008	0.185±0.005
sIRPS2	0.229±0.005	0.236±0.004	0.255±0.008	0.237±0.003	0.241±0.008	0.218±0.010
sIRPS3	0.248±0.006	0.276±0.007	0.278±0.006	0.275±0.003	0.268±0.005	0.243±0.009
sIRPS4	0.234±0.006	0.241±0.006	0.261±0.005	0.248±0.008	0.235±0.009	0.225±0.006
sIRPS5	0.200±0.007	0.215±0.008	0.232±0.004	0.228±0.008	0.215±0.010	0.180±0.005
sIRPS7	0.254±0.007	0.269±0.004	0.263±0.005	0.251±0.003	0.253±0.007	0.227±0.006
sIRPS8	0.218±0.014	0.229±0.008	0.210±0.005	0.221±0.005	0.217±0.006	0.196±0.004
sIRPS9	0.173±0.004	0.223±0.014	0.247±0.008	0.223±0.006	0.193±0.004	0.190±0.006
IRPS	0.172±0.005	0.193±0.003	0.211±0.010	0.197±0.006	0.189±0.005	0.162±0.003

Note: Table 4 presents the absorbance values at 570 nm (A570) of lymphocytes stimulated solely with different concentrations of sIRPS. The data reflect the proliferation response of lymphocytes to each polysaccharide variant. Unstimulated cells served as the negative (cell) control group

Firstly, whether it is sIRPS1~sIRPS9 or IRPS, the lymphocyte proliferation value increases with the increase of EPS concentration. This indicates that the increase in the concentration of EPS has a positive promoting effect on lymphocyte proliferation. For example, the proliferation value of sIRPS1 at a concentration of 0.098 g/mL of EPS is 0.200±0.004, while at a concentration of 1.563 g/mL, its proliferation value rises to 0.220±0.008. Similarly, the proliferation value of IRPS at a concentration of 0.098 g/mL of EPS is 0.172±0.005, while at a concentration of 1.563 g/mL, its proliferation value increases to 0.189±0.005. Secondly, at the same concentration, there are also differences in lymphocyte proliferation values among different sIRPS. For example, when the concentration of EPS is 1.563 g/mL, the lymphocyte proliferation value of sIRPS1 is 0.200±0.004, while the proliferation value of sIRPS3 is 0.248±0.006, and the proliferation value of sIRPS7 is 0.254±0.007. This indicates that there are differences in the sensitivity of different sIRPS to EPS (p<0.05). Once again, the study compares the cell control group: EPS has a significant promoting effect on lymphocyte proliferation (p<0.05 indicates that the result is significant). For example,

the proliferation value of sIRPS1 at a concentration of 1.563 g/mL of EPS is 0.200±0.004, while the proliferation value of the cell control group is 0.185±0.005. This indicates that EPS have a significant promoting effect on the proliferation of lymphocytes in sIRPS1. Table 5 shows the changes in lymphocyte proliferation during synergistic PHA stimulation with sIRPS.

As shown in Table 5, the effects of sIRPS on sIRPS1 to sIRPS9 vary at different concentrations. Under PHA stimulation, the proliferation rate of lymphocytes also varies. Firstly, at a concentration of 1.563 μg/mL, the values of sIRPS1 to SIRPS9 are 0.332, 0.332, 0.307, 0.302, 0.321, 0.326, 0.295, 0.331, and 0.311, respectively. These values are all lower than those under PHA stimulation, indicating that at this concentration, sIRPS has less effect on lymphocyte proliferation than PHA stimulation (p<0.05). However, when the concentration of sIRPS decreases to 0.196 μg/mL, the values of sIRPS1 to sIRPS9 are 0.364, 0.351, 0.321, 0.315, 0.358, 0.342, 0.33, 0.334, and 0.319, respectively. These values are higher than those at a concentration of 1.563 μg/mL, indicating that when the concentration of sIRPS decreases, its proliferation effect on lymphocytes is enhanced. In addition, no matter how the concentration of sIRPS changes, the value under PHA stimulation is always higher than the value of the control group. This indicates that PHA stimulation can significantly enhance the proliferation of lymphocytes. The overall significant changes are shown in Figure 6.

In Figure 6, the effects of sIRPS and PHA stimulation on lymphocyte proliferation are complex, and their effects may be influenced by various factors, including the concentration of sIRPS and the presence of PHA.

Analysis of Antioxidant Activity Test

This section analyzes the scavenging ability of sEPS on hydroxyl radicals. Firstly, research can observe the trend of changes in the hydroxyl radical scavenging ability of different polysaccharide samples at different concentrations. The table shows that as the concentration decreases from 1 mg/mL to 0.0625 mg/mL, and the scavenging ability of different polysaccharide samples shows different trends. The concentration gradient set for the antioxidant experiment is determined by referring to the commonly used range in previous studies, combined with the solubility of the sample and the stability of the color reaction. Currently, it is mainly used for in vitro activity evaluation and has not been directly compared with the physiological concentration in vivo. Vc (1 mg/mL) is used as a positive control in all free radical scavenging assays to evaluate the relative antioxidant capacity of the selenized polysaccharide samples. The Vc solution is treated under the same volume and conditions as the polysaccharide samples, and its absorbance is used to calculate the standard scavenging rate, serving as a reference baseline for comparative analysis. Table 6 shows the data on the scavenging ability of polysaccharides from EPS to hydroxyl radicals.

Table 5: Changes in lymphocyte proliferation under synergistic PHA stimulation of sIRPS

Concentration (μg/mL)	1.563	0.782	0.391	0.196	0.098	PHA	Control
sIRPS1	0.332	0.335	0.349	0.364	0.338	0.305	0.226
sIRPS2	0.332	0.333	0.365	0.351	0.345	0.305	0.225
sIRPS3	0.307	0.305	0.311	0.321	0.301	0.289	0.225
sIRPS4	0.302	0.31	0.324	0.315	0.311	0.283	0.229
sIRPS5	0.321	0.323	0.341	0.358	0.328	0.291	0.224
sIRPS6	0.326	0.333	0.352	0.342	0.343	0.317	0.221
sIRPS7	0.295	0.295	0.32	0.33	0.315	0.286	0.226
sIRPS8	0.331	0.333	0.349	0.334	0.345	0.297	0.23
sIRPS9	0.311	0.315	0.34	0.319	0.319	0.288	0.224

Note: Table 5 presents the absorbance values at 570 nm (A570) of lymphocytes under synergistic stimulation with PHA and various concentrations of sIRPS. The results indicate the enhancement of lymphocyte proliferation due to the combined stimulation. The PHA group served as the positive control, and unstimulated cells were used as the negative (cell) control group

Table 6: Scavenging ability of EPS to hydroxyl radical

Concentration (mg/mL)	1	0.5	0.25	0.125	0.0625
sEPS1	67.89±1.13	33.51±0.82	17.76±1.08	12.66±1.13	3.56±0.50
sEPS2	66.51±0.56	32.12±0.21	14.88±0.27	11.73±0.43	3.28±0.47
sEPS3	67.64±0.87	35.88±0.19	17.43±1.03	9.22±0.95	3.50±0.28
sEPS4	71.25±1.28	41.69±1.22	26.97±0.86	15.66±0.46	6.59±0.41
sEPS5	69.18±1.05	37.94±0.92	17.98±1.08	11.27±0.58	3.41±0.88
sEPS6	68.24±0.88	36.08±0.92	13.86±1.10	5.76±0.34	2.65±0.53
sEPS7	75.50±1.32	43.48±0.89	26.40±0.61	6.19±0.78	5.99±0.78
sEPS8	68.51±0.42	39.12±0.51	17.81±0.51	9.82±0.58	3.34±0.15
sEPS9	68.33±1.67	36.94±1.04	18.22±0.58	8.29±0.97	3.35±0.42
EPS	66.32±0.83	34.88±1.16	12.27±0.96	6.76±0.45	2.63±0.59
VC	98.53±0.49	97.35±0.73	82.98±0.89	34.76±0.81	12.28±0.71

Note: Table 6 shows the scavenging ability (%) of sEPS against hydroxyl radicals at different concentrations. Results indicate that the scavenging rate generally decreases with the reduction of concentration. Vc is used as the positive control to evaluate antioxidant capacity

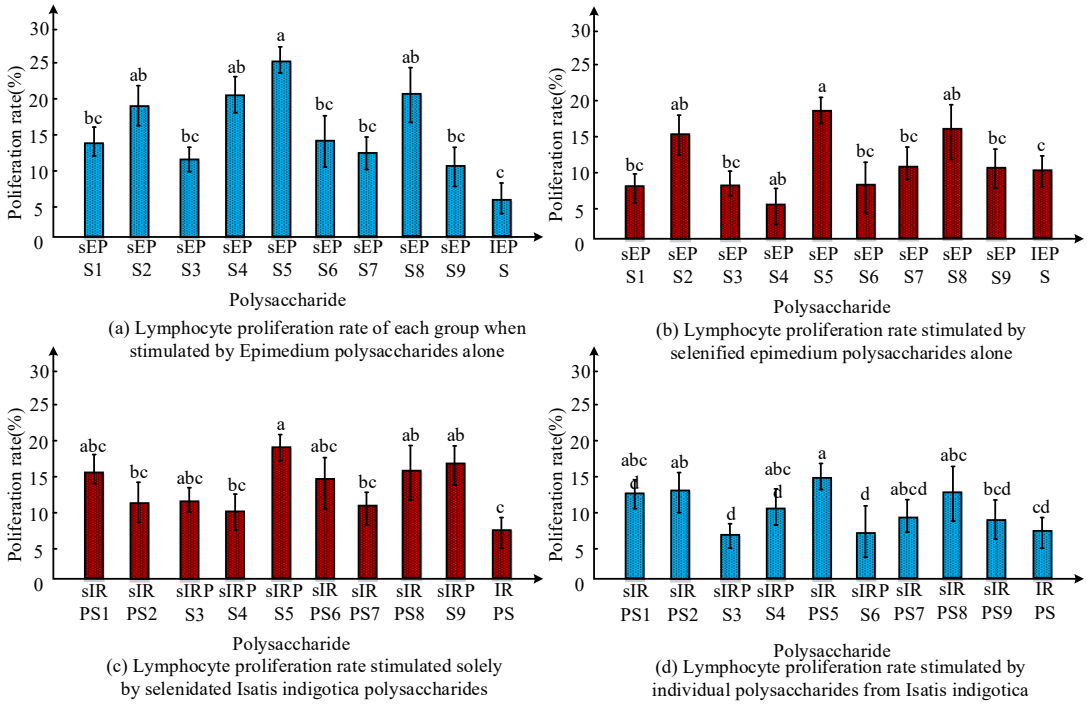

Fig. 6: Significant changes

Note: This figure presents the effects of sEPS and sIRPS on lymphocyte proliferation under different concentrations and stimulation conditions. Panels (a) and (b) show proliferation rates induced by selenized polysaccharides alone, while panels (c) and (d) show the synergistic effects when combined with PHA stimulation. Differences in proliferation rates reflect the immune-enhancing potential of each treatment

In Table 6, for sEPS1 samples, as the concentration decreases, the scavenging ability of hydroxyl radicals gradually weakens, decreasing from 67.89 mg/mL to 3.56 mg/mL. Similarly, the scavenging ability of sEPS2, sEPS3, sEPS5, and sEPS8 samples also shows a similar trend. As the concentration decreases, the scavenging ability of hydroxyl radicals gradually weakens. However, the situation of sEPS4, sEPS6, and sEPS7 samples is slightly different. Although their scavenging ability gradually weakens as the concentration decreases, their scavenging ability is still relatively high at a concentration of 0.0625 mg/mL, at 6.59 mg/mL, 2.65 mg/mL, and 5.99 mg/mL, respectively. This indicates that at lower concentrations, these samples still exhibit significant hydroxyl radical scavenging ability. When comparing the clearance ability of different polysaccharide samples, it is found that sEPS7 samples have the highest clearance ability at all concentrations. At a concentration of 1 mg/mL, the scavenging ability of sEPS7 sample is 75.50 mg/mL, which is much higher than other samples. The sEPS1 sample shows lower clearance ability at all concentrations. In addition, research can also compare the clearance ability of polysaccharide samples with Vc. In the table, even at the lowest concentration, the hydroxyl radical scavenging ability of Vc is still significantly higher than that of all polysaccharide samples. For example, at a concentration of 0.0625 mg/mL, the scavenging ability of Vc is as high as 12.28 mg/mL, while the scavenging ability of sEPS1 is only 3.56 mg/mL. Based on the data provided in the table, the study can conclude that there are significant differences in the hydroxyl radical scavenging ability of different polysaccharide samples at different concentrations. At the same concentration, the scavenging ability of different polysaccharide samples also varies. Compared with Vc, polysaccharide samples have lower scavenging ability. These conclusions indicate that sEPS has a certain scavenging ability on hydroxyl radicals, but their scavenging ability is relatively weaker than that of Vc. Table 7 shows the parameters of the scavenging ability of sIRPS on hydroxyl radicals.

In Table 7, from a concentration of 1 mg/mL to 0.0625 mg/mL, the scavenging ability of sIRPS shows a decreasing trend. As the concentration decreases, the clearance ability gradually decreases. This trend indicates a negative correlation between the scavenging ability of sIRPS and their concentration. Taking sIRPS1 as an example, at a concentration of 1 mg/mL, the clearance ability reaches 29.87, while at a concentration of 0.0625 mg/mL, the clearance ability is only 0.8. As the concentration decreases, the scavenging ability significantly decreases, indicating that the scavenging

ability of sIRPS is positively correlated with its concentration. The higher the concentration, the stronger the scavenging ability. Compared with sIRPS, Vc (ascorbic acid) has a stronger scavenging ability at the same concentration. Taking a concentration of 1 mg/mL as an example, the clearance ability of Vc is 96.24, while the sIRPS1 is only 29.87. This indicates that the scavenging ability of Vc on hydroxyl radicals is much higher than that of sIRPS. Therefore, sIRPS has a certain scavenging ability on hydroxyl radicals, and its scavenging ability increases with the increase of concentration. However, compared to Vc, the scavenging ability of sIRPS is lower. Therefore, Vc may be a more effective antioxidant choice in the process of combating hydroxyl radicals. As the concentration increases, the scavenging ability increases, but its scavenging ability is relatively low. This analysis result can provide important reference for further research on the antioxidant properties of sIRPS. Table 8 shows the scavenging ability of sEPS on ABTS free radicals.

Table 7: Scavenging capacity of sIRPS to Hydroxyl radical

Concentration (mg/mL)	1	0.5	0.25	0.125	0.0625
sIRPS1	29.87	11.72	4.8	2.35	0.8
sIRPS2	31.14	11.45	6.14	3.38	1.14
sIRPS3	26.59	12.47	3.85	1.97	0.54
sIRPS4	41.81	24.58	12.22	5.02	1.54
sIRPS5	34.55	17.82	7.53	2.92	1.04
sIRPS6	28.39	14.97	5.24	2.21	0.86
sIRPS7	45.29	26.39	13	7.03	2.19
sIRPS8	29.98	15.75	7.67	4.24	1.42
sIRPS9	25.76	9.92	3.91	2.01	0.48
IRPS	24.91	10.76	3.45	1.78	0.95
Vc	96.24	97.36	82.58	53.14	36.96

Note: Table 7 presents the scavenging capacity (%) of sIRPS against hydroxyl radicals at various concentrations. The data demonstrate a dose-dependent antioxidant activity. Vc serves as the positive control for comparative analysis

Table 8: Scavenging Ability of sEPS on ABTS Free Radical

Concentration (mg/mL)	1	0.5	0.25	0.125	0.0625
sEPS-1	80.32±1.09	55.34±0.54	43.93±1.02	31.02±0.65b	20.31±0.50
sEPS2	75.67±0.48	51.07±0.62	39.23±0.83	27.12±0.43	17.19±0.46
sEPS3	75.42±0.63	50.87±1.02	41.42±0.59	27.32±0.43	15.23±0.27
sEPS4	81.03±0.83	56.32±0.58	44.87±1.01	31.52±0.79	19.54±0.40
sEPS5	75.56±0.78	49.89±0.98	39.04±0.69	26.35±0.75	15.22±0.72
sEPS6	72.25±0.578	47.09±1.47	36.23±1.10	25.48±0.81	13.86±0.82
sEPS7	82.71±0.87	57.90±0.76	46.63±0.32	33.66±0.78	21.14±0.78
sEPS8	74.28±0.66f	49.54±0.84	25.41±1.40	13.79±0.14	13.79±0.12
sEPS9	77.88±0.75	52.28±0.60	41.15±0.84	28.01±1.00	15.39±0.14
EPS	70.85±1.09	46.38±0.68	35.30±0.57	24.39±0.65	13.46±0.58
Trolox	98.32±0.86	65.42±0.97	35.83±1.53	20.52±1.16	9.98±0.68

Note: Table 8 shows the scavenging ability (%) of sEPS against ABTS free radicals at different concentrations. Data are presented as mean±standard deviation. Trolox is used as the positive control. The results indicate a concentration-dependent antioxidant effect

Table 8 shows the data changes of various indicators under different concentrations observed in the study. At a concentration of 0.0625 mg/mL, the value of sEPS-1 is 20.31±0.50, while the values of sEPS2, sEPS3, sEPS4, and sEPS5 are 17.19±0.46, 15.23±0.27, 19.54±0.40, and 15.22±0.72, respectively. At low concentrations, the values of sEPS-1 and sEPS4 are relatively low, while the values of sEPS2, sEPS3, and sEPS5 are relatively high. This indicates that sEPS may have a strong ability to scavenge ABTS free radicals at low concentrations. Secondly, the numerical changes of the same indicator at different concentrations are compared. Taking sEPS-1 as an example, when its concentration gradually decreases from 1 mg/mL to 0.0625 mg/mL, its value shows a gradually decreasing trend. This indicates that the scavenging ability of sEPS decreases with the decrease of concentration. Furthermore, the study compares and analyzes different indicators at different concentrations. Taking sEPS-1 and sEPS-8 as examples, at a concentration of 0.0625 mg/mL, the value of sEPS-1 is 20.31±0.50, while the value of sEPS-8 is 13.79±0.12. The value of sEPS-1 at this concentration is significantly higher than that of sEPS-8, indicating that sEPS-1 has a significantly stronger ability to scavenge ABTS free radicals than sEPS-8 at this concentration. Finally, the study compares the scavenging ability of sEPS with Trolox. At all concentrations, the values of Trolox are higher than those of sEPS. Taking the data at a concentration of 1 mg/mL as an example, the value of Trolox is 98.32±0.86, while the value of sEPS-1 is

80.32±1.09. Even at the highest concentration, the scavenging ability of sEPS is only about 81.68% that of Trolox. Studies have shown that the scavenging ability of sEPS on ABTS free radicals increases with increasing concentration, but their scavenging ability is still relatively weak compared to Trolox. In addition, at a concentration of 0.0625 mg/mL, the scavenging ability of sEPS may be stronger. These results provide important reference for further research on the scavenging ability of sEPS. Table 9 shows the ABTS free radical clearance rates of the sIRPS groups.

According to Table 9, the overall trend shows that the scavenging rate increases with concentration, indicating a clear dose-dependent effect. Among all samples, sIRPS7 consistently exhibits superior scavenging ability at all tested concentrations, reaching a rate as high as 35.26% at 1 mg/mL, outperforming other variants. This suggests that sIRPS7 may possess a more favorable distribution of active binding sites, possibly due to its selenization degree or structural conformation. In comparison, samples such as sIRPS5 and sIRPS4 also demonstrate strong antioxidant activity at medium to high concentrations (0.5-1 mg/ml), whereas sIRPS1 and sIRPS6 show relatively weaker activity overall. These differences may be attributed to variations in selenium incorporation sites, degree of substitution, spatial conformation, and molecular weight, which in turn affect their radical-scavenging capacity. In addition, compared with the classic antioxidant Trolox, although Trolox has a very high clearance rate (98.32%) at 1 mg/ml, its clearance rate drops to 20.52% at 0.0625 mg/ml, narrowing the performance gap with several sIRPS samples. This indicates that sIRPS still maintain notable antioxidant activity even at lower concentrations. Due to their high molecular weight, good biocompatibility, and safety, these compounds may be more suitable for long-term antioxidant defense. Especially in scenarios requiring chronic intake or multi-target regulation, natural polysaccharide-based antioxidants offer significant advantages for use in health supplements and functional food applications.

Table 9: ABTS free radical clearance rates of sIRPS in each group

Concentration (mg/mL)	1	0.5	0.25	0.125	0.0625
sIRPS1	17.71±1.24	11.70±1.35	5.54±0.51	4.33±0.48	3.03
sIRPS2	24.71±1.10	13.13±0.38	7.35±1.29	5.48±0.61	2.84
sIRPS3	23.49±0.46	14.09±0.40	7.52±1.62	7.03±0.50	3.3
sIRPS4	29.01±0.74	17.96±0.60	9.52±1.01	6.53±0.95	3.87
sIRPS5	31.66±0.99	18.73±1.31	10.62±0.80	10.49±0.80	3.71
sIRPS6	24.34±0.27	12.00±0.88	7.37±0.67	6.34±0.95	2.62
sIRPS7	35.26±1.16	21.17±0.57	13.42±0.97	9.07±0.89	4.69
sIRPS8	26.08±0.27	17.48±1.38	9.29±0.56	9.02±0.71	3.87
sIRPS9	25.49±0.72	15.59±1.58	9.23±0.49	7.09±0.65	3.19
IRPS	17.96	13.31	1.37	6.8	3.21
Trolox	98.32	0.86	65.42	35.83	20.52

Note: Table 9 presents the ABTS free radical clearance rates (%) of sIRPS at various concentrations. Values are shown as mean±standard deviation where available. Trolox is used as the reference antioxidant. The results reveal a concentration-dependent antioxidant capacity across the tested groups

Discussion

This study confirmed that both sEPS and sIRPS exhibited significant immunoenhancing and antioxidant activities in vitro. All experimental data were analyzed using one-way ANOVA followed by LSD post-hoc tests, with statistical significance defined as $p<0.05$, ensuring the reliability of the results. In terms of immune activity, sIRPS3 and sEPS7 significantly promoted PBMC proliferation within the concentration range of 0.098-0.391 mg/ml, with A570 values notably higher than the negative control ($p<0.05$). These findings aligned with the work of Gharibzahedi *et al.* (2022), who reported that polysaccharides with higher sugar content and lower protein contamination exhibited stronger immunostimulatory properties. Similar trends were also observed in the study by Tang *et al.* (2021), where GLPs-stabilized SeNPs induced NO and TNF-α production in macrophages, emphasizing the synergistic potential of selenium and natural polysaccharides in immune regulation.

Under co-stimulation with PHA, both sEPS5 and sIRPS5 showed significantly higher proliferation rates than the PHA-only group ($p<0.05$), indicating their capacity to synergistically enhance immune signaling. This was consistent with the findings of Shabana and Abd El-Sadek (2021), who reported that carbomer-adjuvanted vaccines significantly enhanced humoral immunity in guinea pigs. In addition, Zhang *et al.* (2022) demonstrated that Se-POP-3 from selenium-rich Pleurotus ostreatus activated T-cell proliferation and cytokine secretion, supporting the safety and efficacy of organic selenium polysaccharides in immunomodulation.

In antioxidant assessments, sEPS7 demonstrated the strongest ABTS radical scavenging ability (82.71±0.87% at 1 mg/ml), significantly outperforming sEPS8 (13.79±0.12%, $p<0.01$) and showing a concentration-dependent trend. This result was in agreement with

Angelo *et al.* (2022), who noted that the antioxidant capacity of coffee bean phenolics is closely linked to their polyhydroxy and aromatic structures. Likewise, sIRPS7 exhibited a high hydroxyl radical scavenging rate of 45.29% at 1 mg/ml, significantly higher than that of the IRPS control group (24.91%, $p<0.05$), and surpassed most sEPS samples. This was comparable to the study by Chen *et al.* (2023), where a curcumin-based polyester with hydrophilic domains and phenolic groups exhibited enhanced radical scavenging properties. However, when compared to positive controls such as Vc (96.24%) and Trolox (98.32%), both sEPS and sIRPS demonstrated significantly weaker antioxidant capacity ($p<0.05$), indicating that these polysaccharides may be better suited as daily dietary antioxidants rather than for acute oxidative stress management.

It is worth noting that the sEPS and sIRPS exhibited different strengths in scavenging ABTS and hydroxyl radicals, suggesting that their antioxidant mechanisms may differ. ABTS free radicals were more stable and were commonly used to evaluate the total free radical scavenging ability of water-soluble and fat soluble antioxidants. Hydroxyl radicals had high activity and were the main contributors to DNA and protein damage in the body. In this study, sEPS7 showed a higher scavenging rate in the ABTS system, which may be related to its greater hydroxyl group exposure and better water solubility. In contrast, sIRPS7 demonstrated superior hydroxyl radical scavenging ability, potentially due to its degree of selenization, molecular stability, and targeted reactivity toward highly active radicals. These differences indicated that the two selenized polysaccharides might have complementary applications and could be suited for protecting against different types of oxidative damage.

The study not only confirmed the functional advantages of sEPS and sIRPS in immune enhancement and antioxidant activities but also revealed that higher sugar purity, moderate molecular weight, and specific functional groups (e.g., O–H, C = O) play critical roles in activity expression. These findings support the structure–function paradigm proposed by Gharibzahedi *et al.* (2022) regarding polysaccharide bioactivity. The results also responded to current research trends in functional food development and medicinal applications of selenium-enriched herbal ingredients.

Conclusion

This study established the extraction and selenization procedures for EPS and IRPS and systematically evaluated their immunoenhancing and antioxidant activities in vitro. The experimental results demonstrated that both types of selenized polysaccharides effectively scavenged free radicals and promoted the proliferation of PBMCs across a range of concentrations. Notably, several samples exhibited significant biological activity even at concentrations as low as 0.098 mg/ml. Statistical analysis indicated that the differences between treatment groups and the cell control group were statistically significant ($p<0.05$), with certain samples achieving highly significant levels in hydroxyl and ABTS radical scavenging assays ($p<0.05$). The immunostimulatory effects also displayed a dose-dependent trend. Comparative analysis revealed that sIRPS exhibited superior overall performance in terms of free radical scavenging capacity and PBMC proliferation rate, suggesting greater potential for antioxidant and immunomodulatory applications.

However, this study has certain limitations. Although multiple concentration gradients were tested, a complete dose–response curve was not systematically constructed, and the optimal effective concentration range remained to be clarified. Future research should incorporate more dose–effect indicators and strengthen pharmacodynamic modeling to more comprehensively assess the biological activity of different polysaccharide samples. In addition, it is recommended to conduct in vivo animal experiments to verify its immunomodulatory and antioxidant effects, and further investigate its potential mechanisms. Especially, it can activate classic signaling pathways such as TLR4/NF-κB, regulate the expression of inflammatory cytokines, and evaluate long-term toxicity and efficacy. These efforts will provide a theoretical and data foundation for the development of these polysaccharides as functional foods or botanical therapeutics.

List of Abbreviations

sEPS: selenized Epimedium polysaccharides
sIRPS: selenized Isatis root polysaccharides
ABTS: 2, 2′-azino-bis(3-ethylbenzothiazoline-6-sulfonic acid)
AFS: Atomic Fluorescence Spectrometry
DEAE-52: Diethylaminoethyl Cellulose 52
DMSO: Dimethyl Sulfoxide
DPPH: 2, 2-diphenyl-1-picrylhydrazyl
MTT: 3-(4, 5-dimethylthiazol-2-yl)-2, 5-diphenyltetrazolium bromide
PBMC: Peripheral Blood Mononuclear Cell
PHA: Phytohemagglutinin
RPMI-1640: Roswell Park Memorial Institute Medium 1640
SPSS: Statistical Package for the Social Sciences
UV: Ultraviolet
Vc: Vitamin C

Acknowledgment

Thanks to Jiangsu Vocational Institute of Commerce for all the necessary support in this research.

Funding Information

This paper receives no external funding.

Authors Contributions

Rui Zhang: Investigation and Data Curation.
Jin Li: Formal Analysis.
Jiajia Zhou: Investigation, Formal Analysis, and Visualization.

Ethics

This article does not contain any studies with human participants performed by any of the authors.

Conflict of Interest

The authors declare no conflict of interests.

Data Availability Statements

All data generated or analyzed during this study are included in this published article.

References

Abdel-Moneim, A.-M. E., El-Saadony, M. T., Shehata, A. M., Saad, A. M., Aldhumri, S. A., Ouda, S. M., & Mesalam, N. M. (2022). Antioxidant and antimicrobial activities of Spirulina platensis extracts and biogenic selenium nanoparticles against selected pathogenic bacteria and fungi. *Saudi Journal of Biological Sciences*, *29*(2), 1197–1209. https://doi.org/10.1016/j.sjbs.2021.09.046

Ali, W., Benedetti, R., Handzlik, J., Zwergel, C., & Battistelli, C. (2021). The innovative potential of selenium-containing agents for fighting cancer and viral infections. *Drug Discovery Today*, *26*(1), 256–263. https://doi.org/10.1016/j.drudis.2020.10.014

Angelo, A. F. B., Karime, C. W., James, T. T., Bea Gouanda , T., & Anoubilé, B. (2022). Antioxidant Activity of Aqueous Extracts of Roasted Bean Seeds of Coffea canephora Rubiaceae. *American Journal of Pharmacological Sciences*, *9*(2), 63–68. https://doi.org/10.12691/ajps-9-2-3

Chen, R., Funnell, J. L., Quinones, G. B., Bentley, M., Capadona, J. R., Gilbert, R. J., & Palermo, E. F. (2023). Poly(pro-curcumin) Materials Exhibit Dual Release Rates and Prolonged Antioxidant Activity as Thin Films and Self-Assembled Particles. *Biomacromolecules*, *24*(1), 294–307. https://doi.org/10.1021/acs.biomac.2c01135

Desale, V. J., Mali, S. N., Thorat, B. R., & Yamgar, R. S. (2021). Synthesis, admetSAR Predictions, DPPH Radical Scavenging Activity, and Potent Anti-mycobacterial Studies of Hydrazones of Substituted 4-(anilino methyl) benzohydrazides (Part 2). *Current Computer-Aided Drug Design*, *17*(4), 493–503. https://doi.org/10.2174/1573409916666200615141047

Fan, Y., Zhou, X., & Huang, G. (2022). Preparation, structure, and properties of tea polysaccharide. *Chemical Biology & Drug Design*, *99*(1), 75–82. https://doi.org/10.1111/cbdd.13924

Ge, B., Wang, W., Gao, Y., & Chen, X. (2023). Optimization of extraction of lycopene from carrot and determination of its antioxidant activity. *Journal of Food Measurement and Characterization*, *17*(5), 5497–5505. https://doi.org/10.1007/s11694-023-02046-9

Gharibzahedi, S. M. T., Marti-Quijal, F. J., Barba, F. J., & Altintas, Z. (2022). Current emerging trends in antitumor activities of polysaccharides extracted by microwave- and ultrasound-assisted methods. *International Journal of Biological Macromolecules*, *202*, 494–507. https://doi.org/10.1016/j.ijbiomac.2022.01.088

Kulkarni, K., & Govindaiah, G. (2022). Evaluation of Anti-oxidant properties of some medicinal plant products by ABTS Radical Scavenging Assay. *Research Journal of Science and Technology*, *14*(4), 213–218. https://doi.org/10.52711/2349-2988.2022.00035

Ma, X., Gao, H., Yang, B., Zhao, H., & Zhu, Z. (2022). Huaier Polysaccharide Attenuates Doxorubicin-Induced Acute Cardiotoxicity by Regulating Ferroptosis. *Bulletin of Experimental Biology and Medicine*, *174*(1), 37–42. https://doi.org/10.1007/s10517-022-05644-7

Masood, F., Masood, J., Zahir, H., Driss, K., Mehmood, N., & Farooq, H. (2023). Novel Approach to Evaluate Classification Algorithms and Feature Selection Filter Algorithms Using Medical Data. *Journal of Computational and Cognitive Engineering*, *2*(1), 57–67. https://doi.org/10.47852/bonviewjcce2202238

Ndwandwe, B. K., Malinga, S. P., Kayitesi, E., & Dlamini, B. C. (2021). Advances in green synthesis of selenium nanoparticles and their application in food packaging. *International Journal of Food Science & Technology*, *56*(6), 2640–2650. https://doi.org/10.1111/ijfs.14916

Plermjai, K., Mekprasart, W., Boonyarattanakalin, S., & Boonyarattanakalin, K. (2023). Enhancing Saccharide Extraction from Konjac by Microwave-assisted Acid Hydrolysis. *Thai Journal of Nanoscience and Nanotechnology*, *8*(1), 11–17. https://doi.org/10.55003/tjnn8120232

Shabana, W. S., & Abd EL-Sadek, A. (2021). Effect of Carbomer as an Adjuvant for Enhancement of Immune-Response Against FMD Vaccine. *Journal of Applied Veterinary Sciences*, *6*(2), 27–36. https://doi.org/10.21608/javs.2021.154578

Shi, X.-D., Tian, Y.-Q., Wu, J.-L., & Wang, S.-Y. (2021). Synthesis, characterization, and biological activity of selenium nanoparticles conjugated with polysaccharides. *Critical Reviews in Food Science and Nutrition*, *61*(13), 2225–2236. https://doi.org/10.1080/10408398.2020.1774497

Sun, J., Ren, R., Yao, L., Tong, L., Li, J., Wang, D., & Gu, S. (2024). Preparation, characterization, antioxidant, and hypoglycemic activity of polysaccharide nano-selenium from Fagopyrum tataricum. *Journal of Food Measurement and Characterization*, *18*(9), 7967–7978. https://doi.org/10.1007/s11694-024-02778-2

Tang, L., Luo, X., Wang, M., Wang, Z., Guo, J., Kong, F., & Bi, Y. (2021). Synthesis, characterization, in vitro antioxidant and hypoglycemic activities of selenium nanoparticles decorated with polysaccharides of Gracilaria lemaneiformis. *International Journal of Biological Macromolecules*, *193*, 923–932. https://doi.org/10.1016/j.ijbiomac.2021.10.189

Wang, T., Zhao, H., Bi, Y., & Fan, X. (2021a). Preparation and antioxidant activity of selenium nanoparticles decorated by polysaccharides from *Sargassum fusiforme Journal of Food Science*, *86*(3), 977–986. https://doi.org/10.1111/1750-3841.15605

Wang, X., Wang, Y., Pan, W., Wang, J., & Sun, X. (2021b). Carbon-Dot-Based Probe Designed to Detect Intracellular pH in Fungal Cells for Building Its Relationship with Intracellular Polysaccharide. *ACS Sustainable Chemistry & Engineering*, *9*(10), 3718–3726. https://doi.org/10.1021/acssuschemeng.0c08160

Yang, W., Huang, G., Chen, F., & Huang, H. (2021). Extraction/synthesis and biological activities of selenopolysaccharide. *Trends in Food Science & Technology*, *109*, 211–218. https://doi.org/10.1016/j.tifs.2021.01.028

Zhang, W., & Huang, G. (2022). Preparation, structural characteristics, and application of taro polysaccharides in food. *Journal of the Science of Food and Agriculture*, *102*(14), 6193–6201. https://doi.org/10.1002/jsfa.12058

Zhang, Y., Zhang, Z., Liu, H., Wang, D., Wang, J., Liu, M., Yang, Y., & Zhong, S. (2022). A natural selenium polysaccharide from Pleurotus ostreatus: Structural elucidation, anti-gastric cancer and anti-colon cancer activity in vitro. *International Journal of Biological Macromolecules*, *201*, 630–640. https://doi.org/10.1016/j.ijbiomac.2022.01.101

Zhang, Z., Zhang, Y., Liu, H., Wang, J., Wang, D., Deng, Z., Li, T., He, Y., Yang, Y., & Zhong, S. (2021). A water-soluble selenium-enriched polysaccharide produced by Pleurotus ostreatus: Purification, characterization, antioxidant and antitumor activities in vitro. *International Journal of Biological Macromolecules*, *168*, 356–370. https://doi.org/10.1016/j.ijbiomac.2020.12.070

Zhao, Y., Chen, H., Li, W., He, Q., Liang, J., Yan, X., Yuan, Y., & Yue, T. (2022). Selenium-containing tea polysaccharides ameliorate DSS-induced ulcerative colitis via enhancing the intestinal barrier and regulating the gut microbiota. *International Journal of Biological Macromolecules*, *209*, 356–366. https://doi.org/10.1016/j.ijbiomac.2022.04.028